The International Archives of the Photogrammetry, Remote Sensing and Spatial Information Sciences, Volume XLVIII-M-9-2025
30th CIPA Symposium "Heritage Conservation from Bits:
From Digital Documentation to Data-driven Heritage Conservation", 25–29 August 2025, Seoul, Republic of Korea

Denoising and Voxelization Algorithms for Finite Element Analysis of Cultural Heritage

Sara Gonizzi Barsanti [1], Ernesto Nappi [1], Erika Elefante [1], Anna Manzone [2]

[1] Dept. of Engineering, Università degli Studi della Campania Luigi Vanvitelli, via Roma 29, 81031, Aversa (CE), Italy – sara.gonizzibarsanti@unicampania.it; ernesto.nappi@unicampania.it; erika.elefante@unicampania.it
[2] Conservator Restorer Officer, Head of the Historical and Artistic Heritage Care and Management Service, Reggia di Caserta, Piazza Carlo di Borbone 81100 Caserta (CE), Italy – anna.manzone@cultura.gov.it

Keywords: 3D Point Cloud, Denoising, Voxel, FEA, Cultural Heritage.

Abstract

Reality-based surveys deliver 3D point clouds that can be converted in volumes for FEA. The paper aims at analysing the geometric accuracy for the conversion of 3D point clouds: first step is the denoising of 3D data, then the automatic voxelization for the volumetric models that can be used for structural analyses through Finite element analysis (FEA) process. This work presents an automated pipeline for point cloud denoising and voxelization using Open3D and SciKit-Image. The approach leverages Marching Cubes for surface extraction and exports the results in STL format, ensuring compatibility with CAD and manufacturing systems. This process has been compared to an established one using retopology for the direct conversion of 3D meshes to volumes. The test objects selected for this study are the statue of Moses by Michelangelo, a stool in the Royal Palace of Caserta and a part of a suspension of a Porsche Cayenne. The choice was made considering the increase in geometric complexity of the object, to test the algorithm on objects of different shapes and dimensions. The portion of the suspension was chosen because laboratory data on traction and compression are available for comparison. In this stage, geometrical comparison between the different models have been done to set up the best pipeline for volumetric models for FEA.

1. Introduction

The conservation and the structural integrity of Cultural Heritage can be assessed through the combined use of reality-based 3D models and FEA (Finite Element Analysis). It is possible to transform 3D point clouds obtained through reality-based methods into volumetric data for FEA using different techniques. The most used is NURBS modelling (Shapiro et al., 2011) through CAD environment. The process, even if well established, gives as result a model that is not as accurate as the initial one. To use directly 3D models int FEA, two processes can be used: simplification with retopology (Gonizzi et al, 2022) of the triangular mesh and then export in NURBS volumes, or voxels. Knowing that the starting result of reality-based survey is a point cloud and having the necessity to obtain the most accurate result possible, it is mandatory to check its accuracy. Uncooperative materials or surfaces, poor lighting conditions, reflections, complicated geometries, and limitations in the precision of the instruments can all influence the accuracy of the point cloud, meaning that can add noise to its structure. This noise can be overcome using specific algorithms, to obtain a less noisy data. from this, the process for creating volumes for FEA can be performed. In this paper the process (Fig.1) of denoising point clouds to create volumes has been analysed comparing the results obtained from two different methodologies: (i) denoising point cloud, meshing, retopology and creation of NURBS; (ii) denoising point cloud and voxelization.

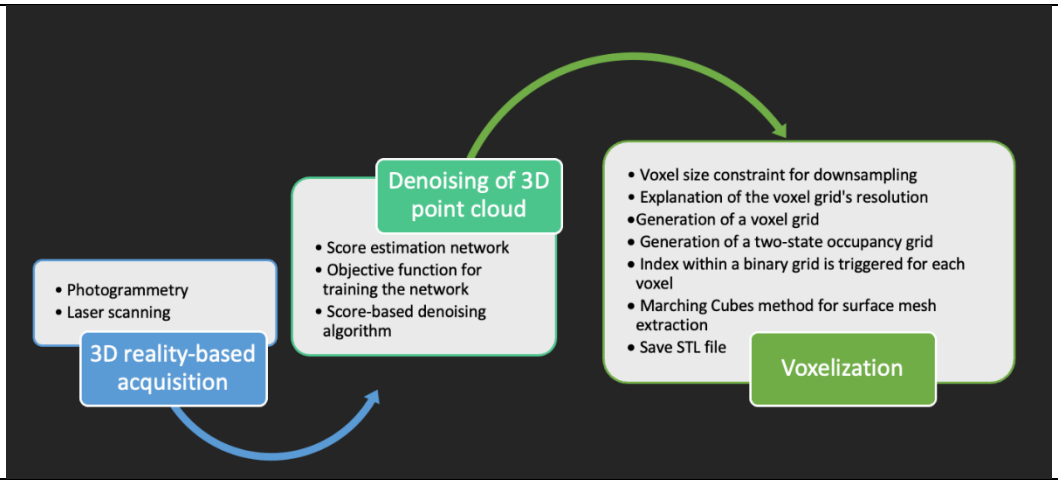

Figure 1. The process followed in this paper (© Gonizzi, Nappi 2025 by the authors, CC BY)

From a literature review, there is no research by now that uses denoising and voxelization algorithms combined for structural analysis of Cultural Heritage. A huge part considers voxelization for object detection (Sun et al, 2022; He et al., 2022) and in medical applications (Ly et al., 2022; Goto et al., 2022). The use of voxelized models for FEA has been investigated in

(Sapozhnikov, Shchurova, 2022) where micro-modelling based on voxel supported the making of a parametric model and in (Doğan, Güllü, 2022) where voxel modelling was used for investigating roof collapsing improving the reconstruction of hollow geometries in FEA software.

1.1 Denoising

Denoising point clouds is a crucial aspect of 3D geometric data processing, as it helps clean it while enhancing the ideal surface. Bilateral filtering (Tomasi et al., 1998) is recognized as a nonlinear technique for smoothing images, and its concepts have been adapted to point clouds (Chen, Shen, 2018; Gonizzi, Nappi, 2025). This approach considers various elements like point position, normal, and colour (Digne, Franchis, 2017). Guided filtering (He et al., 2013) serves as a specialized image filter that operates as an edge-preserving smoothing operator (Han et al., 2018; Gonizzi, Nappi, 2025). Recently, several filtered-based algorithms have leveraged point normals as guiding signals, iteratively refining and adjusting points to align with these estimated normals. Moreover, graph-based denoising techniques consider the input point cloud as a graph and carry out denoising through selected graph filters (Irfan, Magli, 2021; Gonizzi, Nappi, 2025). In this context, patch-based graph representations create graphs from surface patches derived from the point clouds, with each patch functioning as a node (Dinesh et al., 2020). Optimization-driven denoising methods strive to create a denoised point cloud that closely resembles the original input (Xu, Foi, 2021). Deep learning techniques have also made their way into point cloud processing, where denoising typically starts with noisy inputs and aims to establish a mapping that aligns with the ground truth data during an offline phase. These techniques can be categorized into two types: supervised denoising approaches, like those utilizing PointNet (Rakotosaona et al., 2021), and unsupervised denoising methods (Irfan, Magli, 2021; Gonizzi, Nappi, 2025). The implementation of these denoising algorithms has led to notable improvements in geometric precision and reconstruction accuracy (Shitong, Hu, 2021). The enhanced distribution of points in the cloud indicates that the resulting mesh has fewer topological inaccuracies. This advancement is primarily attributed to the denoising algorithm, which effectively minimizes geometric errors and smooths out areas with high noise density. Consequently, the final mesh exhibits reduced noise levels and prevents issues such as intersecting elements or spikes that could undermine the model's surface. While such geometric adjustments may not significantly impact visualization or virtual applications, they can lead to more accurate outcomes or potentially avoid failures in structural finite element analyses.

1.2 Retopology

Retopology (Gonizzi et al., 2022) is a computer graphic technique that permits to create a new mesh layer on a 3D mesh using quadrangular elements instead of triangular ones. This process allows to strongly simplify the mesh because it reconfigures the topology of the triangular mesh since quadrangular elements enhance the organization of the polygonal surface not losing the initial accuracy of the model obtained. The process considers the geometric characteristics and spatial relations among elements and any change in this relation is considered error, hence delated. this process is useful for the subsequent passage in creating a volume from a 3D reality-based mesh since quadrangular elements are more compliant with the creation of NURBS, made of quadrangular patches.
The process involves several stages, each of one possibly introducing inaccuracies and approximations. Obviously, the amount of accuracy is influenced by the number of interventions made to the 3D mesh and the complexity of the object under analysis:

1. Post-processing of the mesh. (closing holes and checking the topology).
2. Retopology (smoothing).
3. Closing holes and checking the topology.
4. NURBS.

1.3 Voxels

Voxels are 3D pixels arranged into voxel grids, which are the 3D counterpart of an image's organized structure. A voxel grid intersects a point cloud or mesh when it is converted to a voxel representation. Then, points in the mesh or point cloud fall into specific voxels. What’s left is a sculpted depiction of the object after these voxels are kept and any others that do not overlap any points are either eliminated or simply wiped out. Both surface-level and full mesh/point cloud volume voxelization are possible. Software such as MeshMixer or Blender can provide a voxelization tool which automatically generate a voxel model from the mesh. This automatic conversion, however, do not allow a strict control of the process and of the parameter, e.g. Blender allows to control only the number of approximated elements by specifying the resolution or detail level of the re-meshed model while MeshMixer builds a watertight solid by converting the object into a voxel representation adjusting only the solid type - fast or accurate – and the volume accuracy with a sliding tool providing a numerical value as the density. It is hence more accurate to use libraries that allow to set all the parameters and control all the steps. Open3D (Zou et al., 2018) offers essential steps that include (i) 3D data structures, (ii) 3D data pro-cessing algorithms, (iii) scene reconstruction, (iv) surface alignment, and (v) 3D visualization. As far as voxelization is concerned, the challenge linked to the modelling of complex geometries, particularly those of cultural heritage artifacts, is that these algorithms tend to oversimplify. A robust algorithm for voxel processing is referenced in (Zou et al., 2018).

2. Materials and Methods

The object selected for the tests were the statue of Moses of the tomb of Julius II in Rome (Fig.2a), a stool held in the Royal Palace of Caserta (Fig.2b) and a part of a suspension of a Porche Cayenn (Fig.2c). This last object was selected because it was possible to have laboratory results of stress analysis as ground truth for comparing the results on the different models.

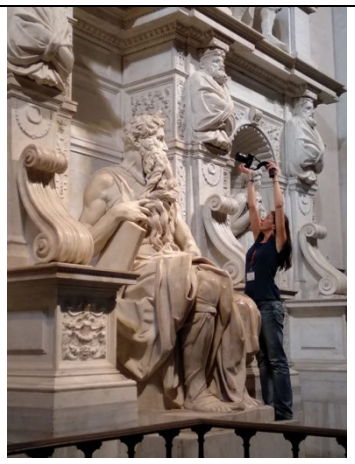

a

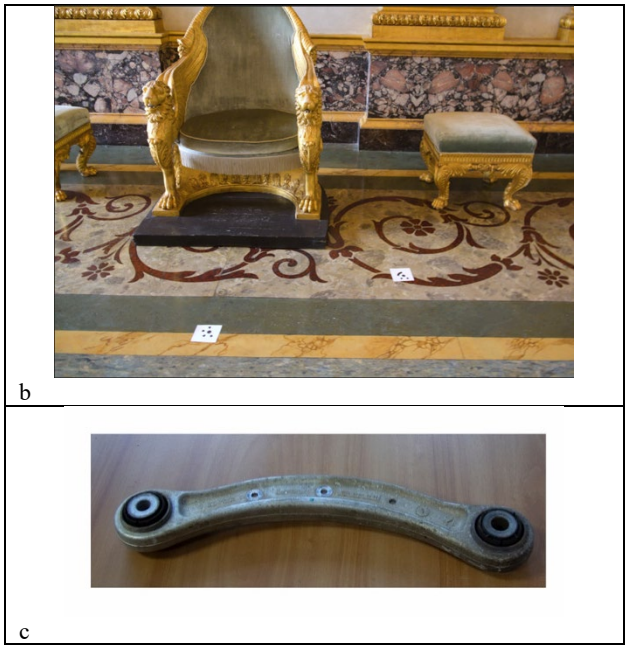

Figure 2. The test objects for this research: a) The statue of Moses; b) the stool in the Caserta; c) the part of the suspension.

The objects have been surveyed with photogrammetry (Table 1), except for the stool for which an integration with a Shining 3D free scan UE pro handheld laser scanner was mandatory to obtain a complete model. This scanner has the possibility to acquire up to 1,850,000 points/s and has a FOV of 600x5500 mm with good coverage for small/medium objects. Its accuracy can reach 0,02 mm and has 7 lines for detailed scans (Fig.3).

OBJECT	CAMERA	PARAMETERS
Moses	Canon 60D + 20mm lens	ISO 250, f/8
Stool	Canon 60D + 18mm lens	ISO 1250, f/3.5
Suspension	Canon 5D + 24mm lens	ISO 400, f/4

Table 1 Camera, lens and parameters for the photogrammetric survey of each object.

It needs to see at least 3 known markers to identify its position in relation to the object surveyed, so specific supports have been 3D printed (in orange in Fig. 3). In addition, some papers covered with markers have been placed below and around the object and other markers were glued on ribbons that were tied around the main part of the object.

The survey of the Mosses was straightforward since it was possible to have the statue completely illuminated by lights on the ceiling of the church, while in the Royal Palace, the illumination was poor. Hence, to prevent the increasing of ISO and since the use of a tripod was not possible, a Godox - LED LED6BI Bicolor 3200K-6500K CRI/TLCI 95 and a Godox LED LD-500W were used (Fig.4a-b) to offer a consistent lighting with different light spectrum following the movement of the camera, so providing an illumination of the part surveyed. The choice between the two devices occurred considering the environmental light: when the place was too dark, the LED LD-500W was used, because it gave a brighter and stronger illumination.

Figure 3. The set-up for the laser scanner survey of the objects in the Royal Palace of Caserta

Figure 4. Godox - LED LED6BI Bicolor 3200K-6500K CRI/TLCI 95 (a) and a Godox LED LD-500W (b) used during the close-range photogrammetry survey.

The two models (Ffig.5a,b)of the stool have been then combined and post processed with Meshmixer and CloudCompare software. To complete the model, different procedures have been used: a manual procedure using Meshmixer and MeshLab software, that allowed to close the holes and fix topology errors, and Design X software, that allowed to manually create a NURBS model from the mesh (Fig. 6c,d).

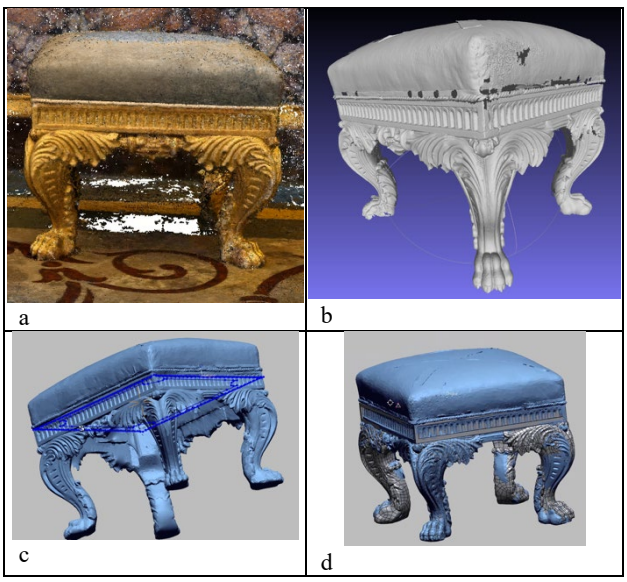

Figure 5. The integration photogrammetric (a) and of laser data (b); the extraction of profiles in the Design X software (c) and the NURBS models obtained with Design X (d)

3. Methodology

3.1 Denoising

The algorithm utilized is among the most significant in recent research. The method introduced by (Shitong, Hu, 2021) features a score-based denoiser within a three-dimensional framework. It leverages deep learning techniques to develop a model capable of identifying the optimal fitting region for each point. This process employs a gradient ascent method to align clusters of outliers with a predicted score function. In essence, the approach mimics an intelligent smoothing process on potential surfaces, relying on a majority voting mechanism (or the density/magnitude of points). The workflow comprises several stages: a score estimation network, the objective function for training the network, and the score-based denoising algorithm. For each object, the original and denoised point clouds have been compare in CloudCompare software considering the Gaussian distribution for both mean and standard deviation along with the C2C (Cloud-to-Cloud) signed distances that just looks for the nearest points and make a comparison (Fig.6, Table 2).

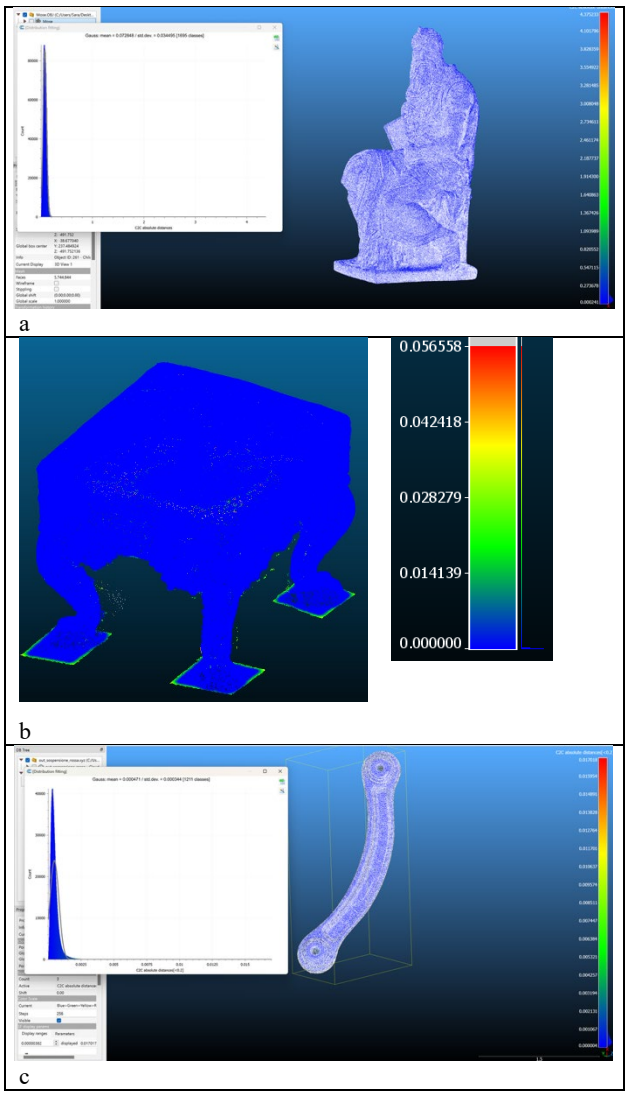

Figure 6. The comparison of raw data and denoised ones: (a) Moses; (b) stool; (c) suspension

The results of the comparison describe perfectly the process used by this algorithm to fix the noise in 3D point clouds: by adapting the points on an ideal surface, cancelling the ones too far from it, the algorithm smooths the point cloud and rearrange the position of points increasing the accuracy with the original object. The standard deviation in the Moses statue, 3 cm) indicates that many points have been recollected and that the noise was strong especially in parts difficult to reach, such as the back of the statue.

OBJECT	Mean (m)	Standard Deviation (m)
Moses	0.073	0.035
Stool	0.0014	0.008
Suspension	0.0005	0.0004

Table 2 For each test object, mean and standard deviation of the comparison between raw data and denoised ones.

3.2 Retopology

For the statue of the Moses, the CloudCompare’s Poisson surface reconstruction (Kazhdan et., 2006) has been used for the creation of a mesh considering that the purpose was to compare the results with raw data.

1. Compute the normal for each point (default parameters).
2. Mesh reconstruction of both noisy and denoised point cloud (leaving parameters on default).
3. Comparison of the two meshes (Fig.7a).
4. Retopology and comparison with raw data.

The goal of this process was to investigate if the denoising algorithm is useful in the meshing process to obtain a more accurate data.

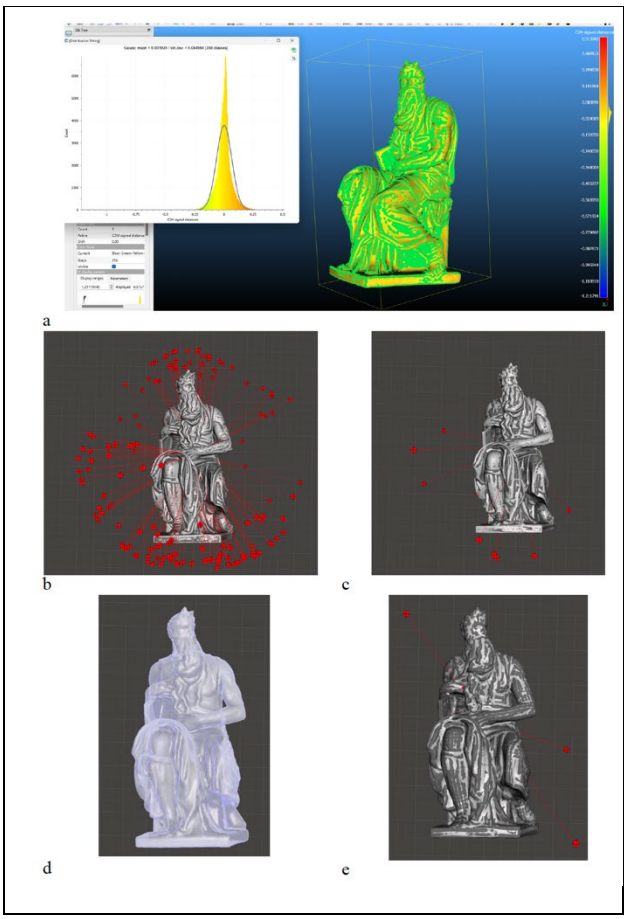

Figure 7. The analysis of 3D meshes and NURBS: (a) comparison of noisy and denoised point cloud; topological errors: (b) not denoised mesh; (c) denoised mesh; (d) denoised retopologised mesh; (e) not denoised retopologised mesh (© 2025 by the authors, CC BY)

Topological errors have been investigated using MeshMixer software (Fig.7b) for both triangular and retopologised meshes using ads starting point noisy and denoised data (Fig.7b-e). The results of the comparison gave a mean of 0.002 and a standard deviation of 0.065 m that are consistent with the results obtained comparing 3D point clouds. What gave an interesting outcome was the analysis of topological errors found by MeshMixer software, e.g. holes, non-manifold polygons, etc. While the triangular mesh derived from noisy data presented many problems, (the red lines in Fig.6b), the one from denoised point cloud showed few (Fig.7c). Applying the retopology process, the mesh from denoised data had no problems at all (Fig.7d) while the one from noisy data only few (Fig.7e). It was also decided to convert the retopologised models into NURBS to create a volume for FEA and the one from the noisy data failed in reconstruction, meaning that the raw data were not good enough to be used directly in the process.

3.3 Voxelization

The denoised data have been then used for the creation of voxel models. For each object, different set-up parameters have been tested to analyse the different results and to try to identify the best values to be used. The first issue to be avoided is the oversimplification that sometimes voxelization imply especially when dealing with complex geometries. For the tests in this research, the algorithm presented in (Baert, 2017) has been used. The open source Open3D library (Zou et al., 2018) with the function voxel_down_sample (self, voxel_size) was used along woith VoxelGrid.create_from_point_cloud function, to directly transform 3D point clouds in voxel models. This library permits the downsampling of the input point cloud to create the volume, following several steps:

- Voxel size to downsample.
- Definition of the resolution of the voxel grid.
- Voxel grid (Figure 8).
- Design of a binary occupancy grid.
- Creation of a resultant index in the binary grid for each voxel.
- Marching Cubes algorithm to extract mesh surface.
- STL file.

The parameter set-up for the process was the voxel_size. The default is set on 0.2 and describes the resolution of the voxel grid. Higher value means higher accuracy but also higher processing time. Then, the Marching Cubes algorithm is used to create the volume with two different set-up parameters:

- level: describes the isovalue for surface extraction. 0.5 value guarantees that the generated mesh follows the midpoint of occupied and unoccupied voxels.
- spacing: certifies precise scaling of the output mesh.


a

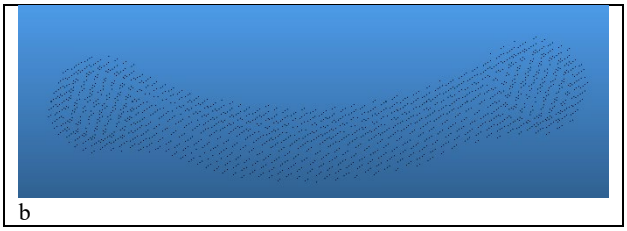
b

Figure 8. The voxel grid pf the statue of Moses (a) and of the suspension (b).

The resultant voxel models have been compared to the original point cloud to analyse possible discrepancies. The results can be seen in Fig. 9a-c and summarized in Table 3. The results are quite in line with the ones obtained comparing raw and denoised point cloud except for the suspension. The reason may lie in the problem related to the modelling of the holes along the body of the object. The survey gave a point cloud with a great amount of noise in that part of the model linked to parts where the data were missing. This may have increased the discrepancies between the models and may have led to a wrong reconstruction of the geometry in the final voxel model.

OBJECT	Mean (m)	Standard Deviation (m)
Moses	0.001	0.05
Stool	-0.0006	0.008
Suspension	0.0001	0.05

Table 3 For each test object, mean and standard deviation of the comparison between raw data and voxel models

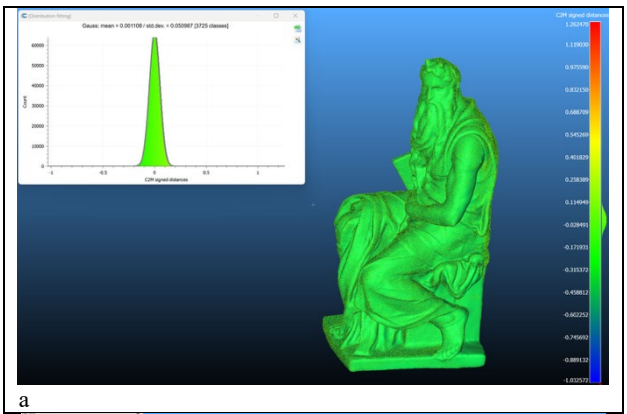
a

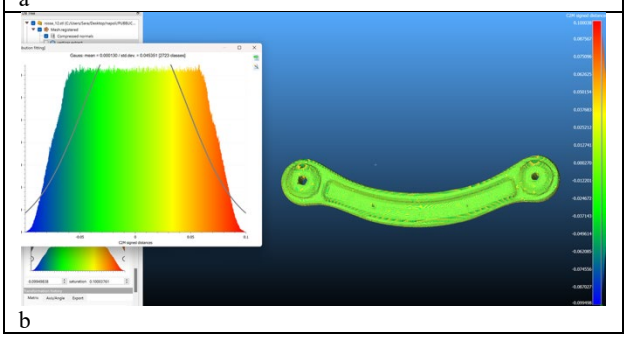
b

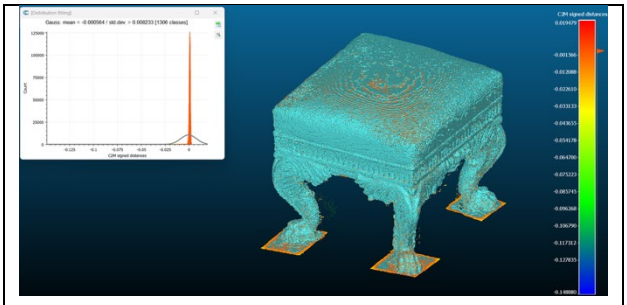

c

Figure 9. The result of the comparison between the raw point cloud and the voxel model: (a) Moses; (b) suspension; (c) stool

3.4 FEA

The part of the suspension of the Porsche Cayenn was firstly tested in laboratory to calculate the strains in tension and compression (Fig. 10). The results obtained, in MPa, were: AE5 Traction 489; AE5 Compression −491; BE6 Traction −345; BE6 Compression 347.

Figure 10. The placement of the sensor to calculate the stress and strain in laboratory on the part of the suspension.

Then, two different retopologised models, created deciding to impose the number of elements of the retopologised models as approximately half and a quarter of their number in the high-resolution model, were imported in FEA (Gonizzi et al., 2024) software to analyse the possible difficulties, errors of uncertainty of measurements that might occur while analysing structural integrity directly on a 3D reality-based model. the values calculated were the maximum principal elastic strain for traction in AE3/AE5 and for compression in BE4/BE6 and the minimum principal elastic strain for compression in AE3/AE5 and for traction in BE4/BE6. (Fig.11). The results were seesawing, some were close to the laboratory test, others, as the one in Fig. 10, gave an error of 15,6%. This may be explained by the difficulties in modelling the holes on the body of the part, that were not perfectly surveyed with photogrammetry. It was necessary to manually open the holes, adding for sure a level of uncertainty that is not completely quantifiable.

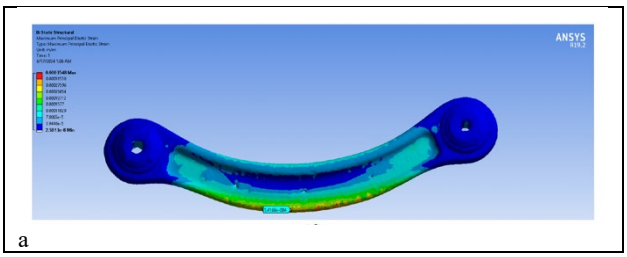

a

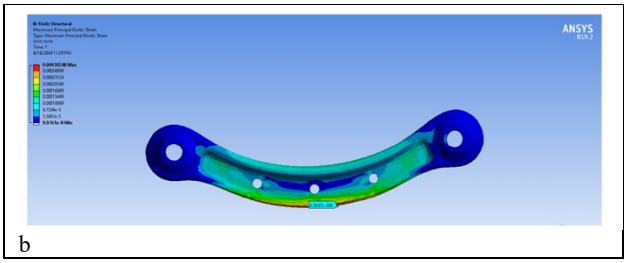

b

Figure 11. One of the results obtained in FEA software: minimum principal elastic strain for compression BE6 for first (a) and second (b) set-up of retopology process.

The results are summarized in Tables 4,5 (Gonizzi et al., 2024).

	AE5 Traction	AE5 Compression	BE6 Traction	BE6 Compression
Lab test	489	−491	−345	347
FEA	363	−354	−326	342
Error%	−25.6	28	5.5	−1.44

Table 4 Comparison of the results of FEA with laboratory tests for the first retopology simplification.

	AE5 Traction	AE5 Compression	BE6 Traction	BE6 Compression
Lab test	489	−491	−345	347
FEA	353	−353	−302	293
Error%	−28	28.1	12.5	−15.6

Table 5 Comparison of the results of FEA with laboratory tests for the second retopology simplification.

Then the voxel model was imported into the software, but it was not possible to proceed with the process since an insurmountable problem occurred: it was not possible to identify parts on the model to impose the force and the boundary conditions, and the meshing, set-up imposing the value of the meshing module close to the dimensions of the elements of the model, failed due to topological problems (Fig.12a,b)

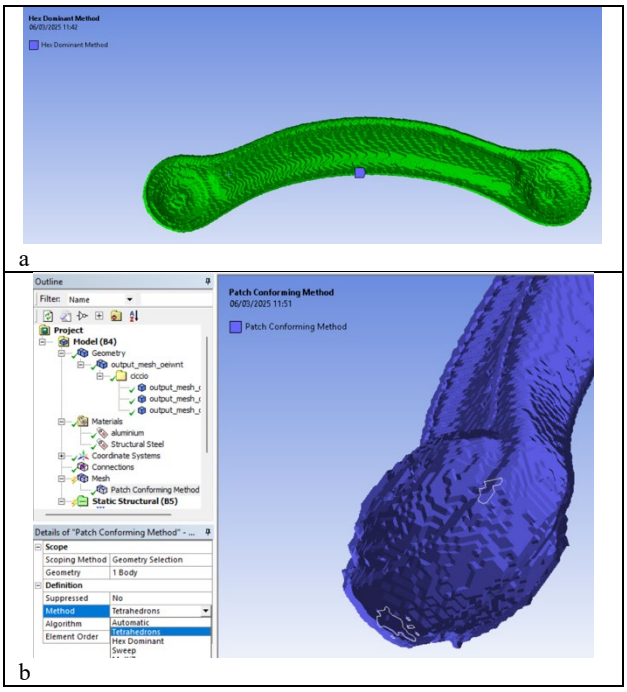

a

b

Figure 12. Problems in FEA software: the process closed all the holes so in was impossible to impose force and boundary conditions (a); the mesh failed because of topological problems (b).

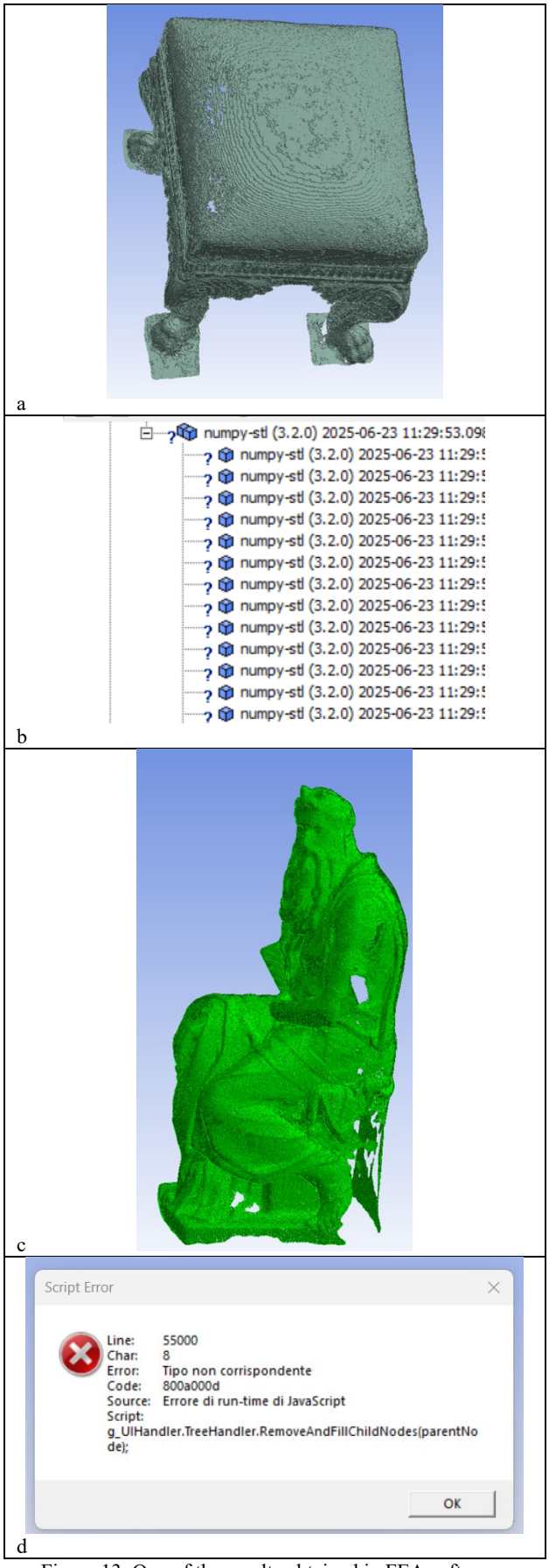

Figure 13. One of the results obtained in FEA software: minimum principal elastic strain for compression BE6

Same problems arose with the other two models (Fig.13a-d). After imposing the parameter, hence, for the Moses, Young modulus 524000 MPa and Poisson ration 0.16 and for the stool (walnut wood) Young’s modulus 9800 MPa e Poisson 0,3, the models have been imported but it was not possible to mesh them. The model of the stool and of the Moses were not complete, holes and missing parts are visible in fig 13a,c. Moreover, the voxel model of the stool was read by the software as it was composed by several parts, failing in the fundamental purpose of the process, that is the creation of a closed volumetric model (Fig.13b). The Model of the Moses, on the other side, was not recognised as a suitable feature to be processed and analysed (fig.13d).

4. Results and conclusions

The use of the denoising algorithm proved the usefulness in term of geometrical accuracy and geometrical reconstruction. The improved scattering of the points in the cloud displayed that the mesh resulted in a geometry with less topological errors avoiding geometric incorrectness with a high intensity of noisy points. This led to a more cleaned mesh, with no intersecting elements or spikes that modify the surface geometry of the model (Gonizzi et al., 2024). This geometric alteration, if on a mesh to be used for visualization or virtual applications, does not substantially influence the results, in structural finite element analyses it can lead, at best, to a further approximation of the results if not even a failure in the process. The present work aimed at analysing the factuality of using precompiled tools and available library for the creation of volumes from 3D reality-based models of object of different shape, geometrical complexity, size, and material. The main problems are related firstly to the input data, that for these software needs to be a mesh while for algorithm are both meshes and 3D point clouds (Gonizzi et al., 2024). If the object is a 3D closed shape, turning its mesh into volume does not add too many approximations, even with automatic tools. On the other hand, if the result is just a surface, the volume needs the thickness of the model to close it properly. This is not something available on custom software. It seemed, considering the results obtained, that the automatic tools are not useful for the creation of accurate volumes is the initial mesh is not a full 3D.

The test of the Open3D library gave optimal results in the creation of the voxel grid from 3D point clouds that are geometrically well defined and correctly structured, while it simplified too much point clouds that presented complex geometry or tiny details. On the other hand, the algorithm was able to voxelise the grids created from point clouds closing the volume although with poor results in terms of details because of the strong approximation of the grid with particularly complex shapes. The same problem was encountered while creating a mesh from the voxel grid with the algorithm (Gonizzi et al., 2024). The reason lies in the Open3D voxelization function "voxel_down_sample" that sometimes seems to suffer from some issues that clearly show a plane that passes through the figure. This artifact seems to be a well-known issue of the library and contributes to provide a bad result in the output of the algorithm. The issue could be related to the calculated normals of the input point cloud, and further investigations will be performed in the future.

Future work will concentrate, analyse and discuss the possible reasons why the results in the voxel modelling were so mediocre. The intention is to test different algorithms and use point clouds of a great variety of objects, different in shape, geometric complexity and dimensions to see if there is an algorithm or a tool that permits to use volumes in FEA for structural analysis starting directly from 3D reality-based point clouds without increasing the intrinsic approximation of the process. The hope

is that testing different algorithms will lead to a better comprehension of the improvements needed to write a script more adaptable to the geometric complexity of the models analysed. It seems that there is not a script or algorithm nor software that is able to provide a level of accuracy needed for the pipeline proposed. Another possibility will be also to previously segment the point clouds and then apply the voxelisation to create a more suitable model for FEA (subdivided in its specific characteristics of material properties). This process, on the other hand, can add other problems and inaccuracy due to the modelling of single parts instead of the complexity of the object as a unique body.
Furthermore, as expected, this procedure works better on single object as statues because they can be modelled as a closed volume filling the inside with voxels. Buildings need a more careful and complex survey step to acquire both the outside and the inside, the cleaning of the point cloud is longer and has to be done carefully to have a proper, complete and accurate 3D reproduction of the structure. Only from this kind of data it will be possible to start the voxelization process.

Acknowledgements

The authors want to thank the Director of the Reggia di Caserta, Dr. Maffei for accepting the collaboration on this project and helping with the survey procedures and Dr Alessandro Greco and Dr Salvatore Cesarano of the Department of Engineering, University of Campania Vanvitelli for the help provided with the laser scanner survey and the modelling of the stool in Desing X.

References

Shapiro, V.; Tsukanov, I.; Grishin, A. Geometric Issues in Computer Aided Design/Computer Aided Engineering Integration. *J. Comput. Inf. Sci. Eng*. 2011, 11, 21005.

Gonizzi Barsanti, S., Guagliano, M., Rossi, A. 2022. 3D Reality-Based Survey and Retopology for Structural Analysis of Cultural Heritage. Sensors; 22(24):9593, MDPI, Basel, Switzerland

Sun, J., Ji, Y.M., Wu, F., Zhang, C., Sun, Y. Semantic-aware 3D-voxel CenterNet for point cloud object detection, Computers & Electrical Engineering, 98, 2022

He, C., Li, R., Li, S., Zhang, L. Voxel set transformer: A set-to-set approach to 3d object detection from point clouds. In Proceedings of the IEEE/CVF conference on computer vision and pattern recognition, 2022, 8417-8427.

Lv, C., Lin, W., Zhao, B. Voxel Structure-Based Mesh Reconstruction From a 3D Point Cloud in IEEE Transactions on Multi-media, 24, 2022, 1815-1829

Goto, M., Abe, O., Hagiwara, A., Fujita, S., Kamagata, K., Hori, M., Aoki, S., Osada, T., Konishi, S., Masutani, Y., Sakamo-to, H., Sakano, Y., Kyogoku, S., Daida, H. Advantages of Using Both Voxel- and Surface-based Morphometry in Cortical Morphology Analysis: A Review of Various Applications, Magnetic Resonance in Medical Sciences, 21, 1, 2022, 41-57

Sapozhnikov, S.B., Shchurova, E.I. Voxel and Finite Element Analysis Models for Ballistic Impact on Ceram-ic-polymer Composite Panels, Procedia Engineering, 206, 2017, 182-187

Doğan, S., Güllü, H. Multiple methods for voxel modeling and finite element analysis for man-made caves in soft rock of Gaziantep. Bull Eng Geol Environ 2022, 81, 23

Tomasi, C., Manduchi, R. Bilateral filtering for gray and color images, in: Sixth International Conference on Computer Vision 1998, pp. 839–846

Chen, H., Shen, J. Denoising of point cloud data for computer-aided design, engineering, and manufacturing, Engineering with Computers 34, 2018, 523–541

Gonizzi Barsanti, S.; Nappi, E. Testing the Effectiveness of Voxels for Structural Analysis. *Algorithms* 2025, 18, 349. https://doi.org/10.3390/a18060349

Digne, J., Franchis, C.D. The bilateral filter for point clouds, Image Processing online, 2017, 278–287

He, K., Sun, J., Tang, X. Guided image filtering, IEEE Transactions on Pattern Analysis, and Machine Intelligence 35 (6) 2013, 1397–1409

Han, X., Jin, J.S., Wang, M., Jiang, W. Guided 3D point cloud filtering, Multimedia tool and Applications 77, 2018, 17397–17411

Irfan, M.A., Magli, E. Exploiting color for graph-based 3d point cloud denoising, Journal of Visual Communication and Image Representation 75, 2021, 103027

Dinesh, C., Cheung, G., Baji´c, I.V. Point cloud denoising via feature graph Laplacian regularization, IEEE Transactions on Image Processing 29, 2020, 4143–4158

Xu, Z., Foi, A. Anisotropic denoising of 3D point clouds by aggregation of multiple surface-adaptive estimates, IEEE Trans-actions on Visualization and Computer Graphics 276, 2021, 2851–2868

Rakotosaona, M.J., La Barbera, V., Guerrero, P., Mitra, N.J., Ovsjanikov, M. Pointcleannet: Learning to denoise and remove outliers from dense point clouds. In Computer graphics forum, Vol. 39, No. 1, 2021, 185-203.

Shitong, L., Hu, W. Score-based point cloud denoising Proceedings of the IEEE/CVF International Conference on Computer Vi-sion, Montreal, QC, Canada, 2021, 4563-4572

Zhou, Q.Y., Park, J., Koltun, V. 2018. Open3D: A modern library for 3D data processing. arXiv 2018, arXiv:1801.09847.

Kazhdan, M., Bolitho, M., Hoppe, H. Poisson surface reconstruction. In Proceedings of the fourth Eurographics Symposium on Geometry Processing, Vol. 7, 2006

Baert J., Cuda voxelizer: A gpu-accelerated mesh voxelizer. https://github.com/Forceflow/cuda_voxelizer, 2017. 4

Gonizzi Barsanti, S.; De Finis, R.; Nobile, R. Integration of Finite Element Analysis and Laboratory Analysis on 3D Models for Methodology Calibration. Sensors 2024, 24, 4048. https://doi.org/10.3390/s24134048

Gonizzi Barsanti, S.; Marini, M.R.; Malatesta, S.G.; Rossi, A. Evaluation of Denoising and Voxelization Algorithms on 3D Point Clouds. Remote Sens. 2024, 16, 2632 https://doi.org/10.3390/rs16142632